Electronic Supplementary Material (ESI) for ChemComm.

- Supporting Information -

Theoretical perspective on the reaction mechanism from arylpentazenes to arylpentazoles: new insights into the enhancement of *cyclo*-N_5 production.

Guanghua Ren,[a, b, †] Runze Liu,[a, b, †] Panwang Zhou,[c, ‡] Chaoyang Zhang,[d]
Jianyong Liu[a, ‡] and Keli Han [a]

[a] State Key Laboratory of Molecular Reaction Dynamics, Dalian Institute of Chemical Physics, Chinese Academy of Sciences, Dalian 116023, P. R. China.

[b] University of the Chinese Academy of Sciences, Beijing 100049, P. R. China.

[c] Institute of Molecular Sciences and Engineering, Shandong University, Qingdao 266235, P. R. China.

[d] Institute of Chemical Materials, China Academy of Engineering Physics (CAEP), Mianyang, Sichuan 621900, P. R. China.

[†] These authors contribute to this work equally.

[‡] Corresponding author: beam@dicp.ac.cn; pwzhou@sdu.edu.cn.

Index:

1. Computation details

All geometry optimizations were performed using the M06-2X-D3[1] functional with def-TZVP basis set. The nature of the optimized stationary points were characterized by frequency calculations at the same level of theory that all equilibrium states have no imaginary frequency and transition states have only sole imaginary frequency. The intrinsic reaction coordinate (IRC) paths were traced in both forward and backward directions for all transition state geometries. Solvent effects of water (ε = 78.35) were implicitly taken into account by means of solvation model based on density (SMD) method developed by Truhlar's group.[2] Benchmark studies of MP2/aug-cc-pVDZ optimizations were carried out in the following part to validate our DFT level geometries. Furthermore, in order to obtain more accurate electronic energies and reaction barriers, single point calculations for all the optimized structures were performed at DLPNO-CCSD(T)[3]/aug-cc-pVTZ[4] level. Charge information was obtained by natural population analysis (NPA) method.[5] All geometry optimizations were performed using Gaussian 16[6] package and DLPNO-CCSD(T) calculations were carried out using ORCA 4.0[7].

The Gibbs free energy barrier was calculated to evaluate the reaction barrier. The free energy of compounds in solution equals the gas-phase free energy plus the solvation free energy:

$$G = G_{gas} + G_{solvation} \tag{1}$$

The gas-phase free energy is evaluated as:

$$G_{gas} = (E_{gas} + E_{gas}^{\upsilon_0}) + \Delta PV - TS_{gas} \tag{2}$$

with $E_{gas}^{\upsilon_0}$ denotes the zero-point energy correction and E_{gas} equals the electronic energy plus the thermal correction by translational, rotational and vibrational movements:

$$E_{gas} = E_{gas}^{e} + (E_{gas}^{t} + E_{gas}^{\upsilon} + E_{gas}^{r}) \tag{3}$$

and entropy:

$$S_{gas} = S_{gas}^{e} + S_{gas}^{t} + S_{gas}^{v} + S_{gas}^{r} \tag{4}$$

Solvation free energy is calculated based on SMD model as described by Truhlar *et. al.*[8]:

$$G_{solvation} = E_{solv}^{e} - E_{gas}^{e} \tag{5}$$

where E_{solv}^{e} and E_{gas}^{e} are electronic energy calculated under SMD solvation model and gas-phase, respectively. Thermal corrections and entropy contributions to Gibbs free energy were calculated at 298.15 K and 1 atm condition.

2. The decomposition process of different *para*-substituted arylpentazoles

As scheme S1 shows, the free energy barriers for the decomposition of *para*-substituted arylpentazoles are calculated at the SMD/M06-2X-D3/def-TZVP level for geometry optimization followed by single point energy calculations through DLPNO-CCSD(T)/aug-cc-pVTZ method. The benchmark results are reported in Table S1.

Scheme S1

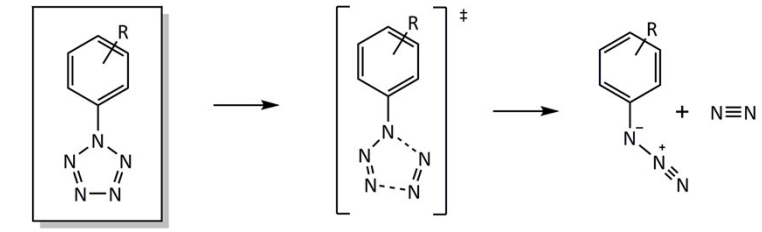

	0	1	2	3	4	5	6	7
R	H	OH	$O(CH_3)$	$O(CH_3)_2$	$N(CH_3)_2$	CN	NO_2	SO_3^-

Table S1 Reaction barriers of decomposition of *para*-substituted arylpentazoles **0-7**

(kcal/mol)	**0**	**1**	**2**	**3**	**4**	**5**	**6**	**7**
ΔG_{sol}	21.7	22.4	22.3	22.3	22.1	21.1	20.9	21.6
ΔG_{gas}	18.7	19.2	19.4	19.6	19.0	17.5	17.3	20.5

The transition geometries of OH and NO_2 substituted arylpentazoles are compared with the ones from the theoretical research by Carlqvist *et al.* (J. Phys. Chem. A 2004, 108, 7463-7467), in which the geometry optimization is carried out at the B3LYP/6-31+g* level.

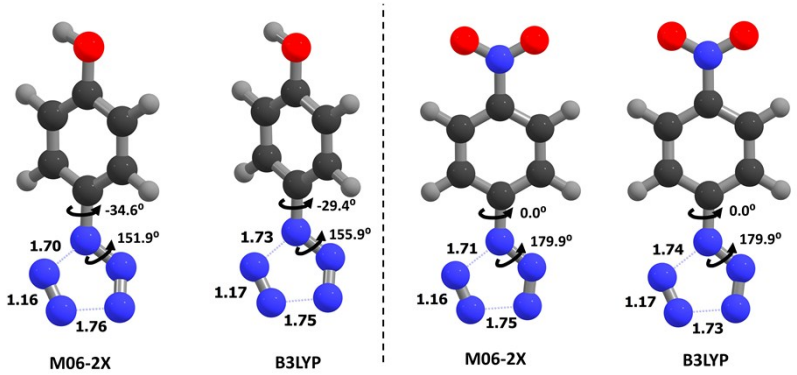

Fig. S1 Transition state geometry for the decomposition of OH and NO_2 substituted arylpentazole obtained at the M06-2X/def-TZVP and B3LYP/6-31+g* level

3. Benchmark studies on geometry optimization

To ensure that the M06-2X-D3 method can reasonably describe our target geometries and the forming and breaking of NN bonds that involved in this work needs further explored. Hence, seven key geometries: ***trans-cis***, ***trans-trans*** and transition state geometries ***ts*1**, ***ts*4**, ***ts*5**, ***ts*6** and ***ts*7** (Fig. 1 and Fig. 3) were selected for the benchmark studies. The corresponding structures are displayed in Scheme S2. Geometry optimizations were performed using the DFT methods (M06-2X, B3LYP, PBE0, wB97XD, B2PLYP) with def-TZVP basis set and the Møller–Plesset perturbation (MP2) method with aug-cc-pVDZ basis set. We employed D3 dispersion correction for the DFT methods to better evaluate the weak interactions. Single point energy calculations at DLPNO-CCSD(T)/aug-cc-pVTZ level were then carried out for all the stationary points. The outcomes are given in the following tables.

Scheme S2

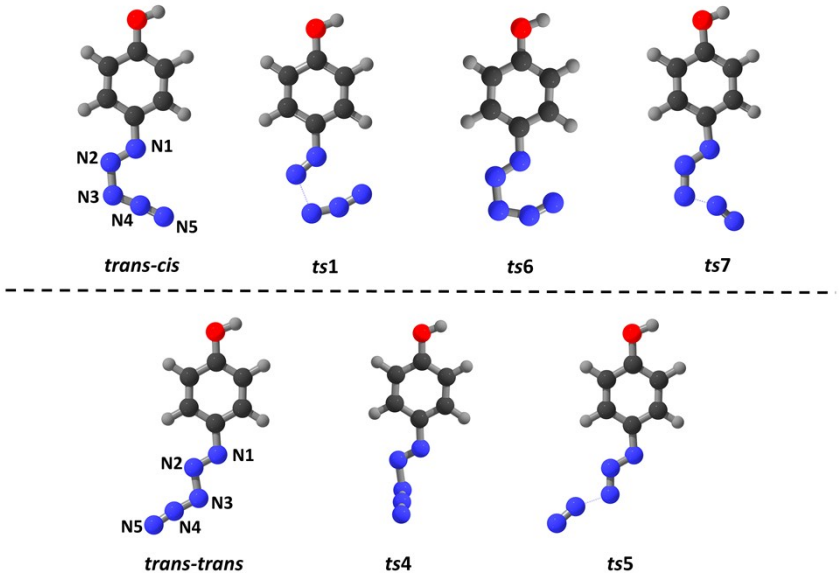

Table S2 The optimized geometry of ***trans-cis*** and energies relative to M06-2X

(Å)	N1-N2	N2-N3	N3-N4	N4-N5	ΔE (kcal/mol)
M06-2X	1.23	1.40	1.26	1.11	0.0
B3LYP	1.24	1.42	1.25	1.12	-0.3
PBE0	1.24	1.40	1.25	1.12	0.3
wB97XD	1.23	1.40	1.25	1.11	0.1
B2PLYP	1.25	1.42	1.26	1.13	0.2
MP2	1.28	1.41	1.28	1.15	1.2

Table S3 The geometry of the transition state ***ts*1** and the reaction barrier of the ***trans-cis*** formation

(Å)	**N1-N2**	**N2-N3**	**N3-N4**	**N4-N5**	**N5-N1**	**ΔG (kcal/mol)**
M06-2X	1.16	1.80	1.20	1.14	2.54	5.8
B3LYP	1.18	1.73	1.21	1.14	2.76	5.8
PBE0	1.17	1.77	1.20	1.15	2.53	5.1
wB97XD	1.16	1.79	1.20	1.14	2.51	5.5
B2PLYP	1.20	1.67	1.23	1.15	2.65	5.7
MP2	1.22	1.66	1.25	1.16	2.64	4.5

Table S4 The geometry of the transition state ***ts*6** and reaction barrier of *cyclo*-N_5 formation from ***trans-cis***

(Å)	**N1-N2**	**N2-N3**	**N3-N4**	**N4-N5**	**N5-N1**	**ΔG (kcal/mol)**
M06-2X	1.21	1.41	1.30	1.13	2.23	4.7
B3LYP	1.22	1.47	1.28	1.14	2.36	5.0
PBE0	1.22	1.43	1.27	1.13	2.38	4.7
wB97XD	1.21	1.43	1.28	1.13	2.31	4.9
B2PLYP	1.22	1.49	1.27	1.15	2.36	4.7
MP2	1.25	1.45	1.31	1.16	2.27	4.1

Table S5 The geometry of the transition state ***ts*7** and reaction barrier of losing N_2 from ***trans-cis***

(Å)	**N1-N2**	**N2-N3**	**N3-N4**	**N4-N5**	**N5-N1**	**ΔG (kcal/mol)**
M06-2X	1.24	1.28	1.48	1.09	3.40	4.2
B3LYP	1.25	1.28	1.44	1.11	3.48	3.7
PBE0	1.24	1.27	1.46	1.10	3.47	3.9
wB97XD	1.24	1.27	1.47	1.10	3.44	4.0
B2PLYP	1.26	1.28	1.45	1.12	3.46	4.5
MP2	1.28	1.27	1.51	1.14	3.46	3.6

Table S6 The optimized geometry of ***trans-trans*** and the energies relative to M06-2X

(Å)	**N1-N2**	**N2-N3**	**N3-N4**	**N4-N5**	**ΔE (kcal/mol)**
M06-2X	1.23	1.40	1.25	1.11	0.0
B3LYP	1.24	1.42	1.24	1.12	-0.2
PBE0	1.24	1.40	1.24	1.12	0.2
wB97XD	1.23	1.41	1.25	1.11	0.1
B2PLYP	1.25	1.42	1.25	1.13	-0.4
MP2	1.27	1.41	1.28	1.15	0.8

Table S7 The geometries of the transition state ***ts*4** and the reaction barrier from ***trans-trans*** to ***trans-cis***

(Å)	**N2-N3**	**N2-N3**	**N3-N4**	**N5-N5**	**D(N1-N2-N3-N4)**	**ΔG (kcal/mol)**
M06-2X	1.23	1.47	1.24	1.13	86.41	8.6
B3LYP	1.23	1.50	1.23	1.13	83.97	8.0
PBE0	1.23	1.47	1.22	1.13	84.85	8.1
wB97XD	1.22	1.47	1.23	1.12	84.80	8.6
B2PLYP	1.23	1.50	1.23	1.14	85.44	7.9
MP2	1.26	1.50	1.26	1.16	88.52	7.9

Table S8 Geometries of the transition state of ***ts*5** and the reaction barrier of losing N_2 of ***trans-trans***

(Å)	**N1-N2**	**N2-N3**	**N3-N4**	**N4-N5**	**ΔG (kcal/mol)**
M06-2X	1.27	1.26	1.65	1.10	19.5
B3LYP	1.27	1.26	1.60	1.10	19.8
PBE0	1.26	1.24	1.59	1.10	20.3
wB97XD	1.26	1.25	1.62	1.09	19.8
B2PLYP	1.28	1.26	1.62	1.11	19.8
MP2	1.30	1.26	1.65	1.14	19.7

4. Theoretical investigation on the concerted cycloaddition for arylpentazole formation

Our calculations with M06-2X-D3/def-TZVP method for the arylpentazole formation gives a stepwise process with the ***trans-cis*** intermediate generates before cyclization. In order to verify the reliability of this conclusion, we performed a relaxed potential energy scan with the bond length R1 and R2 as collective variables (shown in Scheme S3) using the MP2-based B2PLYP functional with def-TZVP basis set.

Scheme S3

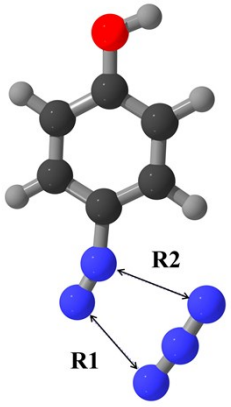

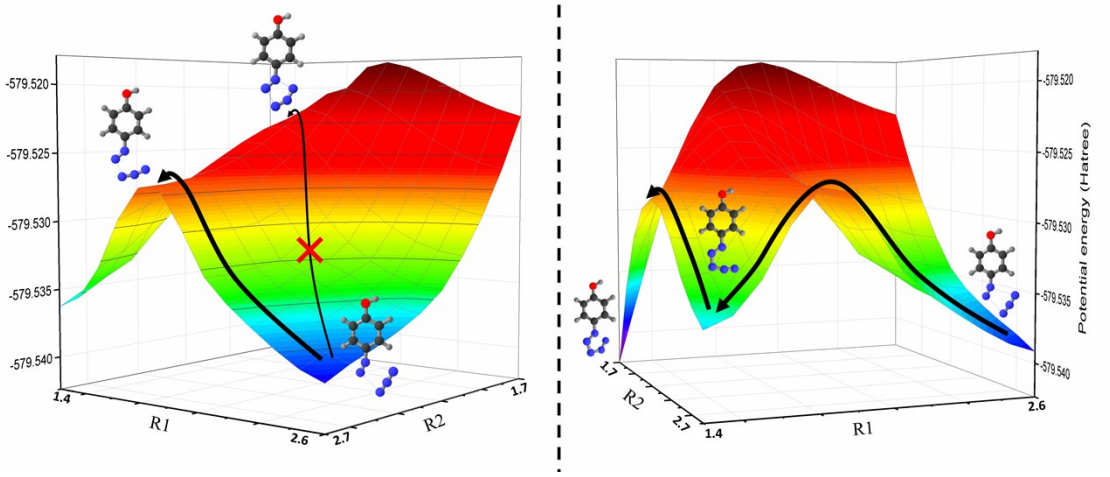

Fig. S2 Potential energy surface as a function of N-N bonds R1 and R2

The starting optimized geometry is shown in Scheme S3, and the scanning step is set as 0.1 Å. The potential energy surface with R1: 2.6-1.4 Å and R2: 2.7-1.7 Å covers the region of saddle points from aryldiazonium and azide reactions. It can be seen from Fig. S2, the formation of arylpentazole through a concerted cycloaddition mechanism is energetically unfavorable, and tends to fall to the state that forms the ***trans-cis***. Therefore the route to arylpentazole prefers a stepwise process relative to the concerted cycloaddition. So differing from the arylpentazole decomposition process, in which the

breaking of N1-N5 and N3-N4 bond is concerted and leads to the N_2 production, the formation process of arylpentazole is stepwise, which involves the generation of arylpentazene intermediate before cyclisation. The following schematic view (Scheme S4) summarized the formation and decomposition of arylpentazole.

Scheme S4

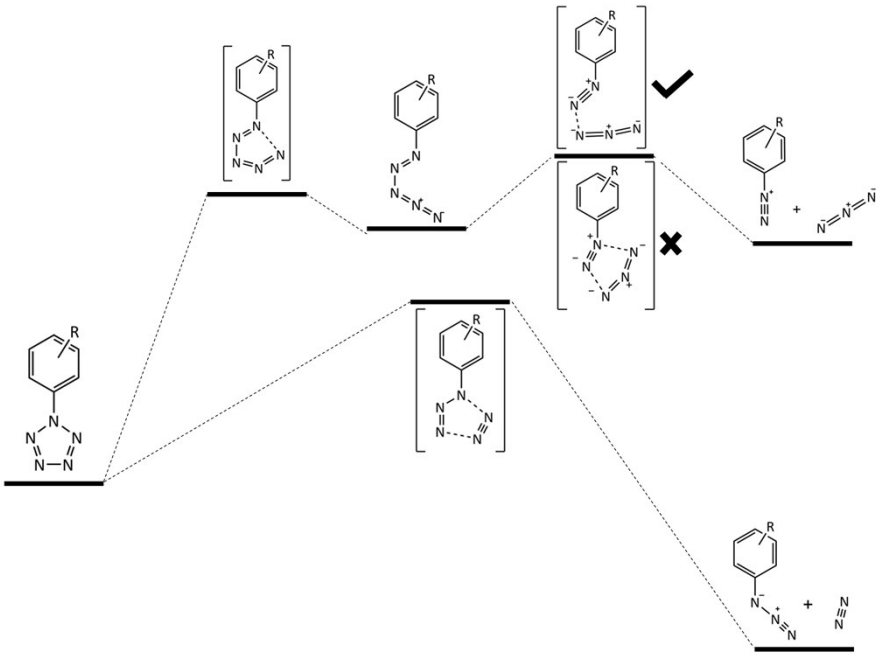

5. Benchmark studies on solvent model

To mimic the experimental liquid-phase reaction, the implicit solvation model based on density (SMD) method was employed in the calculation. Considering that the experimental condition is a mixed polar solvent including water, methanol as well as THF and the ratios change with different experiments. Hence, to evaluate the different solvent effects of SMD model, we have performed benchmark studies for solvents: water, methanol and THF for the reaction barriers of ***trans-cis*** formation, cyclization to pentazole and N_2 loss processes. The calculations are performed at M06-2X-D3/def-TZVP level. As reported in Table S3, the reaction barrier deviations of ΔG_1, ΔG_2 and ΔG_3 using methanol and THF compared with water are displayed in $\Delta\Delta G_1$ to $\Delta\Delta G_3$ columns. As shown in Table S3 the discrepancies of reaction barriers vary from 0.01 to -0.64, which has little influence on the reaction barrier as well as

the general mechanism. Therefore we have employed water as solvent for all the computations in this work.

Table S9 Unit of ***trans-cis*** to ***ts***7: Hatree; Unit of $\Delta\Delta G_1$ to $\Delta\Delta G_7$: kcal/mol

	Water	Methanol	THF
trans-cis	-580.390670	-580.385983	-580.381789
ts1	-580.377433	-580.373098	-580.367894
ts6	-580.383050	-580.378348	-580.374371
ts7	-580.379109	-580.375199	-580.371246
$\Delta\Delta G_1$	-	-0.22	0.42
$\Delta\Delta G_6$	-	0.01	-0.13
$\Delta\Delta G_7$	-	-0.49	-0.64

6. Additional figures and tables.

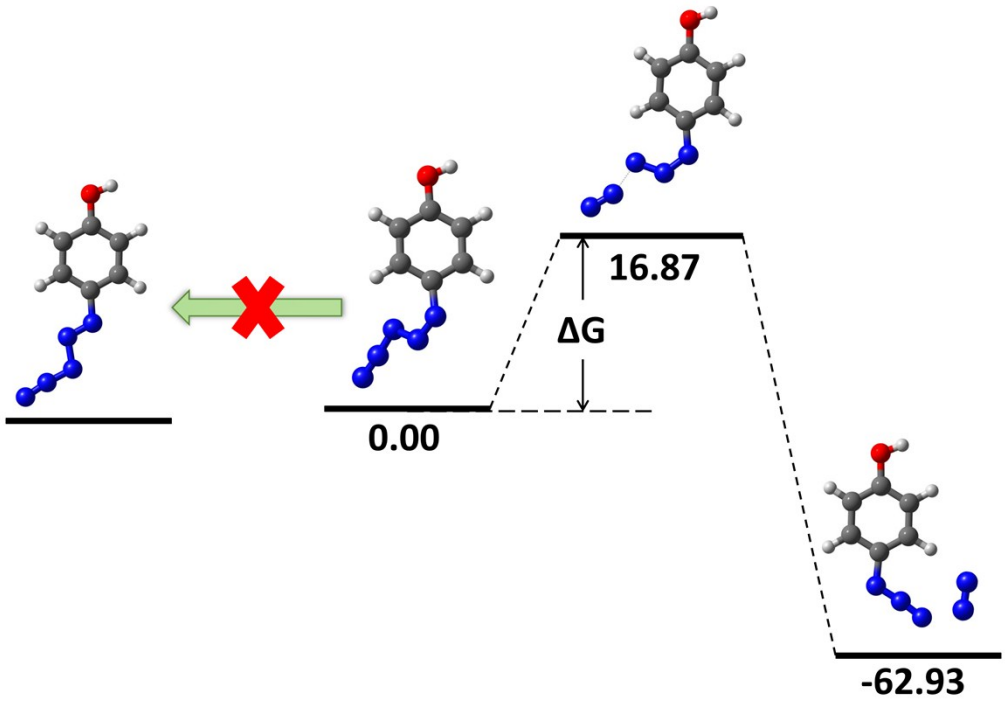

Fig. S3 Reaction pathways for ***cis-trans*** isomerization and N_2 loss process.

Table S10 Gibbs free energy barriers for all reaction processes of different *para*-substituted arylpentazoles.

	ΔG_1	$\Delta G_1'$	ΔG_2	$\Delta G_2'$	ΔG_3	$\Delta G_3'$	ΔG_4	$\Delta G_4'$	ΔG_5	ΔG_6	ΔG_7
0	7.36	6.18	16.36	16.00	8.05	4.32	7.95	6.69	17.91	3.10	3.80
1	8.09	5.83	17.18	14.40	11.02	2.52	8.57	7.27	19.51	4.69	4.19
2	8.48	5.97	16.54	15.75	10.16	2.01	8.61	6.94	19.83	4.23	3.23
3	8.42	5.96	16.24	15.81	10.06	2.06	8.83	6.80	20.51	4.02	3.46
4	12.40	4.20	20.78	11.62	12.62	1.25	7.14	5.85	20.28	4.17	4.68
5	4.03	7.38	13.70	18.27	5.71	6.59	9.06	7.72	17.29	4.32	2.31
6	3.51	7.25	14.81	19.52	6.24	7.29	9.11	7.81	16.86	3.70	1.71
7	5.38	6.53	14.41	18.23	6.93	5.17	8.56	6.87	18.06	4.15	2.72

The corresponding substituents and reaction barriers are as following:

0: no substituents on phenyl ring; **1**: hydroxyl; **2**: methoxy; **3**: ethoxy; **4**: dimethylamino; **5**: cyano; **6**: nitro; **7**: deprotonated sulfonyl.

ΔG_1, ΔG_2 and ΔG_3: reaction barriers for the formation of ***trans-cis***, ***trans-trans*** and ***cis-trans*** pentazenes, respectively;

$\Delta G_1'$, $\Delta G_2'$ and $\Delta G_3'$: reaction barriers for the decomposition of ***trans-cis***, ***trans-trans*** and ***cis-trans*** pentazenes into aryldiazonium and azide.

ΔG_4: reaction barrier for isomerization from ***trans-trans*** to ***trans-cis*** configurations; and $\Delta G_4'$ denotes the reaction barrier for the reverse process.

ΔG_5: reaction barrier for the loss of N_2 from ***trans-trans*** configurations;

ΔG_6: reaction barrier for forming *cyclo*-N_5 from ***trans-cis*** configurations;

ΔG_7: reaction barrier for the loss of N_2 from ***trans-cis*** configurations.

Table S11 The sum of NPA charge population on N_5 groups of the ***trans-cis***, ***ts*6** and *cyclo*-N_5 configurations for molecule from **1** to **7**.

	0	**1**	**2**	**3**	**4**	**5**	**6**	**7**
trans-cis	-0.178	-0.202	-0.203	-0.204	-0.236	-0.147	-0.135	-0.160
ts6	-0.215	-0.238	-0.239	-0.239	-0.274	-0.178	-0.162	-0.194
cyclo-N_5	-0.298	-0.305	-0.305	-0.306	-0.320	-0.278	-0.271	-0.286

Table S12 The sum of NPA charge population on N_5 groups of the ***trans-cis***, ***ts***6 and *cyclo*-N_5 configurations for molecule from **1a** to **1h**.

	1a	**1b**	**1c**	**1d**	**1e**	**1f**	**1g**	**1h**
trans-cis	-0.209	-0.206	-0.203	-0.205	-0.169	-0.163	-0.159	-0.156
ts6	-0.245	-0.243	-0.239	-0.240	-0.201	-0.195	-0.191	-0.188
cyclo-N_5	-0.309	-0.307	-0.309	-0.305	-0.285	-0.281	-0.278	-0.275

Table S13. The sum of NPA charge population on N_5 groups of the ***trans-cis***, ***ts***6 and *cyclo*-N_5 configurations for deprotonated anions from **1'** to **1h'**.

	1'	**1a'**	**1b'**	**1c'**	**1d'**	**1e'**	**1f'**	**1g'**	**1h'**
trans-cis	-0.305	-0.321	-0.337	-0.319	-0.327	-0.265	-0.260	-0.277	-0.247
ts6	-0.344	-0.359	-0.374	-0.353	-0.364	-0.300	-0.297	-0.313	-0.284
cyclo-N_5	-0.349	-0.356	-0.360	-0.356	-0.357	-0.329	-0.326	-0.332	-0.319

Optimized Cartesian coordinates of selected key structures

Optimized ***trans-cis*** of **1** at its equilibrium state

N	4.16911700	1.24497000	0.00034800
N	3.69893300	0.23987800	-0.00022700
N	3.26178200	-0.94208000	-0.00011400
N	1.27662200	0.06581300	0.00009200
N	1.86284300	-1.01678400	0.00005100
C	-0.13975100	-0.00352600	0.00004000
C	-0.87130900	-1.19430400	-0.00008900
C	-0.80236700	1.21892600	0.00011700
C	-2.25034500	-1.15196700	-0.00012800
H	-0.36034300	-2.14747800	-0.00015300
C	-2.18696300	1.26696100	0.00007700
H	-0.22240500	2.13328400	0.00020600
C	-2.90906300	0.07910500	-0.00004700

H	-2.83517800	-2.06283800	-0.00022200
H	-2.71131200	2.21511900	0.00013800
O	-4.27265400	0.05821700	-0.00010600
H	-4.61581900	0.96241900	0.00001200

Optimized ***trans-cis*** of **1** at its transition state to the cyclization

N	3.10766400	1.38966300	-0.00014900
N	3.64317200	0.39189400	-0.00003900
N	3.42629900	-0.88706500	0.00009800
N	1.36790600	-0.00213600	0.00000300
N	2.02122300	-1.02635800	0.00011400
C	-0.04621900	-0.04612100	0.00000000
C	-0.77345100	-1.23745700	-0.00007500
C	-0.69929200	1.18023100	0.00005600
C	-2.15257300	-1.19190800	-0.00006900
H	-0.25904800	-2.18910600	-0.00013300
C	-2.08299400	1.22827800	0.00006600
H	-0.11575200	2.09235500	0.00010200
C	-2.80747900	0.04071400	-0.00000200
H	-2.73879200	-2.10171900	-0.00012800
H	-2.60606400	2.17701700	0.00011500
O	-4.17005500	0.02357800	-0.00000300
H	-4.51170500	0.92842700	0.00002600

Optimized ***trans-cis*** of **1** at its transition state to the loss of N_2

N	4.50614900	1.09125300	-0.07663600
N	3.72153100	0.33024900	-0.02253200
N	3.13936900	-1.03223200	0.06602600
N	1.25420000	0.11330900	0.00232500
N	1.86118700	-0.96957100	0.06614500
C	-0.16287200	0.03039300	0.00083000
C	-0.88249400	-1.16561800	-0.03983500
C	-0.84638800	1.24106800	0.03068300
C	-2.26482100	-1.14315700	-0.03987600
H	-0.36010300	-2.11252200	-0.07088100

C	-2.23306700	1.26914500	0.03011500
H	-0.28248500	2.16517600	0.05805000
C	-2.94121600	0.07456500	-0.00579800
H	-2.83410800	-2.06353700	-0.07203600
H	-2.76860100	2.21101100	0.05498600
O	-4.31057700	0.03668500	-0.01083000
H	-4.66199100	0.93696100	0.01251100

Optimized ***trans-trans*** of **1** at its equilibrium state

N	4.88932700	-0.94622800	0.00015100
N	4.03190400	-0.23907600	0.00009400
N	3.16185300	0.66122800	-0.00010300
N	1.02277800	0.92544100	-0.00029300
N	1.89493400	0.05893200	-0.00028100
C	-0.30946600	0.43568100	-0.00013800
C	-0.65834100	-0.91800400	-0.00026300
C	-1.30402500	1.40749400	0.00011700
C	-1.98847600	-1.28433700	-0.00010800
H	0.10957700	-1.67960600	-0.00048900
C	-2.64139200	1.04554000	0.00027700
H	-1.01980000	2.45228300	0.00019700
C	-2.98106700	-0.30249200	0.00016000
H	-2.27823300	-2.32729100	-0.00021300
H	-3.42178200	1.79734500	0.00048100
O	-4.27804100	-0.72552200	0.00029200
H	-4.87440100	0.03607600	0.00044300

Optimized ***trans-trans*** of **1** at its transition state to reverting to ***trans-cis***

N	-4.44722400	0.15650800	1.21225800
N	-3.84769100	0.00168300	0.28027000
N	-3.26546500	-0.17021700	-0.79277800
N	-1.16980300	0.43726100	-0.41485600
N	-1.86753200	-0.55547500	-0.54660400
C	0.21670200	0.19703000	-0.21941400
C	0.78414400	-1.07144100	-0.08390100

C	1.01653600	1.33450600	-0.16360200
C	2.14577800	-1.19221100	0.10085300
H	0.16268900	-1.95605800	-0.11797100
C	2.38227300	1.21854500	0.01926800
H	0.55559500	2.30874500	-0.26645800
C	2.94541200	-0.04698600	0.15191500
H	2.60477400	-2.16765500	0.21156300
H	3.01866100	2.09250800	0.06347900
O	4.29117200	-0.12000100	0.33534200
H	4.56784500	-1.04251100	0.42789800

Optimized ***trans-trans*** of **1** at its transition state to the loss of N_2

N	-5.00084200	-1.06767600	-0.13989200
N	-4.04757000	-0.54235000	-0.07802600
N	-3.06057200	0.77252400	0.07342600
N	-0.94300600	1.17241200	0.10809300
N	-1.88287700	0.33703800	0.02235400
C	0.34397500	0.56925700	0.06218600
C	0.58264800	-0.80382900	0.13917300
C	1.42206000	1.44144100	-0.04522400
C	1.87684200	-1.29102900	0.08712000
H	-0.24502200	-1.49416600	0.23921500
C	2.72217600	0.95951000	-0.09547900
H	1.23434000	2.50688000	-0.09635100
C	2.94811800	-0.40914500	-0.02927500
H	2.07107800	-2.35460500	0.14753700
H	3.56114200	1.64027700	-0.18223800
O	4.21070900	-0.94535600	-0.07032200
H	4.86193900	-0.23640600	-0.15826600

Optimized ***cis-trans*** of **1** at its equilibrium state

N	4.42077000	-1.02696000	0.53570300
N	3.38655600	-0.65345300	0.36798100
N	2.19164700	-0.33474700	0.21825200
N	1.03619100	1.43742400	-0.55747800

N	2.15255000	0.97680600	-0.35963100
C	-0.17763200	0.72875800	-0.30524700
C	-0.42384700	-0.56425600	-0.76676500
C	-1.18934600	1.45204100	0.31571200
C	-1.66590500	-1.13841400	-0.56762800
H	0.34329100	-1.11179500	-1.29583400
C	-2.42200700	0.86579300	0.55029200
H	-1.00047900	2.47099000	0.62940200
C	-2.65913300	-0.43057500	0.10561100
H	-1.87811100	-2.13625400	-0.92951200
H	-3.20783400	1.41363100	1.05679000
O	-3.85960200	-1.05511600	0.29343000
H	-4.46682200	-0.46921500	0.76606500

7. References

1. S. Grimme, J. Antony, S. Ehrlich and H. Krieg, *J. Chem. Phys.*, 2010, **132**, 154104.
2. A. V. Marenich, C. J. Cramer and D. G. Truhlar, *J. Phys. Chem. B*, 2009, **113**, 6378-6396.
3. C. Riplinger and F. Neese, *J. Chem. Phys.*, **2013**, 138, 034106.
4. E. Papajak, J. Zheng, X. Xu, H. R. Leverentz and D. G. Truhlar, *J. Chem. Theory Comput.*, **2011**, 7, 3027-3034.
5. A. E. Reed, R. B. Weinstock and F. Weinhold, *J. Chem. Phys.*, **1985**, 83, 735-746.
6. M. Frisch, G. Trucks, H. Schlegel, G. Scuseria, M. Robb, J. Cheeseman, G. Scalmani, V. Barone, G. Petersson and H. Nakatsuji, *Gaussian, Wallingford*, *CT*, **2016**.
7. F. Neese, *Wiley Interdiscip. Rev.: Comput. Mol. Sci.*, 2018, **8**, e1327.
8. R. F. Ribeiro, A. V. Marenich, C. J. Cramer and D. G. Truhlar, *J. Phys. Chem. B*, 2011, **115**, 14556-14562.